HHS Public Access

Author manuscript

Biol Psychiatry. Author manuscript; available in PMC 2021 January 15.

Published in final edited form as:

Biol Psychiatry. 2020 January 15; 87(2): 174–184. doi:10.1016/j.biopsych.2019.06.010.

Parsing the Heterogeneity of Brain Metabolic Disturbances in Autistic Spectrum Disorder

Joseph O'Neill,
Division of Child and Adolescent Psychiatry, Semel Institute For Neuroscience, University of California Los Angeles, Los Angeles, CA

Ravi Bansal,
Institute for the Developing Mind, Children's Hospital Los Angeles, Los Angeles, CA; Keck School of Medicine at the University of Southern California, Los Angeles, CA

Suzanne Goh,
Rady Children's Hospital, University of California San Diego, San Diego, CA

Martina Rodie,
School of Medicine, Dentistry & Nursing, University of Glasgow, Glasgow, Scotland

Siddhant Sawardekar,
Institute for the Developing Mind, Children's Hospital Los Angeles, Los Angeles, CA; Keck School of Medicine at the University of Southern California, Los Angeles, CA

Bradley S. Peterson
Institute for the Developing Mind, Children's Hospital Los Angeles, Los Angeles, CA; Keck School of Medicine at the University of Southern California, Los Angeles, CA

Abstract

BACKGROUND: Despite rising prevalence of autistic spectrum disorder (ASD) its brain bases remain uncertain. Abnormal levels of *N*-acetyl-compounds (NAA), glutamate+glutamine (Glx), creatine+phosphocreatine (Cr), or choline-compounds (Cho) measured by proton magnetic resonance spectroscopy (MRS) suggest that neuron or glial density, mitochondrial energetic metabolism, and/or inflammation contribute to ASD neuropathology. The neuroanatomic distribution of these metabolites could help evaluate leading theories of ASD. But most prior MRS studies had small samples (all $n < 60$, most $n < 20$), interrogated only a small fraction of brain, and avoided assessing effects of age, sex, and IQ.

Primary corresponding author: Joseph O'Neill, Ph.D., Division of Child & Adolescent Psychiatry, UCLA Semel institute For Neuroscience, 760 Westwood Plaza, Los Angeles, CA 90024; joneill@mednet.ucla.edu, (responsible for the manuscript from submission through acceptance). Second corresponding author: Bradley S. Peterson, M.D., Institute for the Developing Mind, Children's Hospital Los Angeles, 4650 Sunset Blvd, Los Angeles, CA 90027; bpeterson@chla.usc.edu.
From the Division of Child and Adolescent Psychiatry (JON), Semel Institute For Neuroscience, University of California Los Angeles, Los Angeles, CA; Institute for the Developing Mind (RB, SS, BSP), Children's Hospital Los Angeles, Los Angeles, CA; Keck School of Medicine (RB, SS, BSP) at the University of Southern California, Los Angeles, CA; Rady Children's Hospital (SG), University of California San Diego, San Diego, CA; School of Medicine, Dentistry & Nursing (MR), University of Glasgow, Glasgow, Scotland.

METHODS: We acquired near-whole-brain MRS of NAA, Glx, Cr, and Cho in 78 ASD and 96 typically developing (TD) children and adults, rigorously evaluating effects of diagnosis and severity on metabolites, as moderated by age, sex, and IQ.

RESULTS: Effects of ASD and its severity included reduced levels of multiple metabolites in white matter and perisylvian cortex and elevated levels in posterior cingulate, consistent with white-matter and social-brain theories of ASD. Regionally, both slower and faster decreases of metabolites with age were observed in ASD *vs.* TD. Male-female metabolite differences were widely smaller in ASD than TD. ASD-specific decreases in metabolites with decreasing IQ occurred in several brain areas.

CONCLUSIONS: Results support multifocal abnormal neuron or glial density, mitochondrial energetics, or neuroinflammation in ASD, alongside widespread starkly atypical moderating effects of age, sex, and IQ. These findings help parse the neurometabolic signature for ASD by phenotypic heterogeneity.

Keywords

Autism; Age; Sex; Intelligence; Symptom domains; Magnetic resonance spectroscopy

The ever-surging prevalence of autistic spectrum disorder (ASD) constitutes a public health crisis (1), underscoring the urgency of improved understanding of the neural bases of ASD to inform prevention and treatment. Leading models (mirror neurons, social brain, theory-of-mind,…) ascribe ASD to disturbances throughout the brain (in perisylvian cortex, cingulate, white matter, amygdala,…). These loci can be probed--and models thereby tested--for neurochemical dysfunction using proton magnetic resonance spectroscopy (MRS). MRS assays metabolites such as *N*-acetyl-compounds (NAA), glutamate+glutamine (Glx), creatine+phosphocreatine (Cr), and choline-compounds (Cho). MRS findings in ASD (2,3) have resembled model predictions in being neuroanatomically dispersed, but findings have been variable and poorly replicated, likely because of differences in methods and inadequate accounting for the heterogeneity of ASD (in symptoms, age, sex, IQ,…) To address this heterogeneity, the present study examined a large, well-characterized sample of ASD and typically developing (TD) children and adults that permitted assessment of between-group differences and modifying effects of age, sex, IQ, and ASD symptoms on MRS metabolites using state-of-the-art acquisition and analysis with multiplanar chemical shift imaging (MPCSI). Unlike single-voxel MRS, MPCSI does not readily permit use of short echo-time (TE) and water-referenced quantitation, but it does enable simultaneous wide sampling of brain regions implicated in ASD at high spatial-resolution (~1 cc) in tolerable scantimes.

MATERIALS AND METHODS

Participants

For recruitment, diagnosis, and inclusion/exclusion see (4) and Supplemental Methods. Briefly, 78 individuals with ASD (DSM-IV autistic disorder, Asperger disorder, or pervasive developmental disorder) aged 5–60 (Table 1) participated. The institutional review board of the New York State Psychiatric Institute approved the study and written informed consent was obtained. Assessments included the Autism Diagnostic Interview–Revised (ADI-R)(5)

and, in 66 ASD participants, the Autism Diagnostic Observation Schedule (ADOS)(6). The ADOS returned a Total Score and subscores for Restricted and Repetitive Behaviors and Social Affect symptoms. In 62 ASD and 67 TD participants, ASD symptoms were evaluated with the Social Responsiveness Scale (SRS)(7) yielding a Total Score and subscores for Social Awareness, Social Cognition, Social Communication, Social Motivation, and Restricted Behaviors. Participants with genetic or metabolic abnormalities, history of neurologic injury, recent seizures, contraindications to MRI, or inability to comply with procedures were excluded. In the ASD sample, 26 participants were taking one or more psychotropic medications (Table 1), 52 were taking no medication.

Ninety-six unmedicated TD controls participated after a clinical interview including the Kiddie Schedule for Affective Disorders and Schizophrenia for children or the Structured Clinical Interview for DSM-IV Axis I Disorders for adults. Individuals with current or previous psychiatric or neurologic disorder were excluded. All controls scored below threshold for ASD on the SRS. The full-scale intelligence quotient (FSIQ) was assessed (68 ASD, 93 TD) using the Wechsler Abbreviated Scale of Intelligence. ASD and TD samples did not differ significantly in sex, age, or socioeconomic status (Table 1), but mean FSIQ was 5.9% lower in ASD ($p = 0.046$). We opted not to balance groups for IQ since low IQ is a frequent, and very high IQ an occasional, feature of ASD and a broad IQ range was desired. By design, SRS scores were higher in the ASD sample ($p < 10^{-6}$).

MR Acquisition

MRI and proton MRS were acquired as described (4, also see Supplemental Methods). Briefly, data were collected at 3T (GE Signa) with an 8-channel surface coil. Whole-brain T1-weighted MRI was obtained using 3D spoiled gradient-recall with 0.98×0.98×1.0 mm^3 voxels. The T1 was used to prescribe MPCSI and to segment the brain into gray and white matter. An in-plane high-resolution "localizer" MRI was acquired in register with MPCSI with voxels 0.98×0.98×10 mm^3. The localizer was used to normalize MPCSI data into a common template brain space. MRS was acquired in 6 axial-oblique slabs parallel to the anterior commissure-posterior commissure plane (AC-PC): one slab below, one containing and four above the AC-PC (Figure 1). We acquired water-suppressed MPCSI with TR/TE=2800/144 ms, voxels 10×10×10 mm^3 and outer-volume lipid suppression.

MR Post-Processing

MR data were processed as described (4,8–9 and Supplemental Methods). Briefly, the brain was extracted from the T1-volume, warped into a cross-participant template and segmented into gray and white matter. After time-domain preprocessing, MPCSI data were Fourier-transformed and loaded into the inhouse 3DiCSI software package which identified brain-internal MPCSI voxels. Spectra were fit for NAA, Glx, Cr, Cho, and lipids using Gaussian-Lorentzian curves and least-squares. Areas under the curves estimated metabolite concentrations in each voxel. We quality controlled the data by inspecting each spectrum, rejecting spectra with lipid contamination, insufficient water suppression, lack of separation between Cr and Cho, or linewidth >12 Hz. We computed background noise as the standard deviation of the part of the real spectrum free from metabolite signal. We generated a

spectroscopic image for each metabolite as the ratio of peak area to noise for each voxel, accounting for variations in receiver and transmitter gain.

We corrected each voxel of each participant's spectroscopic images for partial-voluming (variable gray-*vs.* white-matter content across MPCSI voxels) and for the MPCSI point-spread function (dispersion of MR signal into neighboring voxels). For each MPCSI voxel and metabolite we used linear regression to estimate the concentration of that metabolite in gray and white matter using the levels in neighboring voxels and their proportions of gray and white matter. We resampled metabolite levels from low-resolution MPCSI to the high-resolution T1 during spatial normalization. This entailed warping the MPCSI volume for each participant onto the T1 template. We then coregistered each metabolite image onto the template using the T1 and the localizer.

Statistical Analyses

For all metabolite-level analyses we conducted hypothesis testing in each voxel. To control for false positives we applied False Discovery Rate (FDR) at FDR = 0.05; *p*-values surviving FDR were color-coded on statistical parametric maps on the T1-template. Effects of diagnosis on metabolites were evaluated across the combined sample with a multiple linear-regression model that included age, sex, and FSIQ. Effects of symptom severity on metabolites were assessed in the ASD sample using a model that included age and sex. This was done for ADOS and SRS Total Scores and for each subscale. Effects of age on metabolites were evaluated in the combined sample with a model that included age, sex, diagnosis, and an age-by-diagnosis interaction. The interaction was evaluated to identify where in the brain diagnosis effects differed by age. In follow-up analysis, we assessed effects of age separately in the ASD and TD samples using a model that included sex. Effects of sex on metabolites were assessed in the combined sample using a model that included age, sex, diagnosis, and a sex-by-diagnosis interaction. The interaction identified where in the brain group differences varied by sex. In follow-up, we assessed sex effects on metabolites separately in the ASD and TD samples using a model that included age. Given the higher incidence of ASD in males than females, we compared metabolites between the ASD and TD groups using male participants only and a model that included age. Effects of FSIQ on metabolites were assessed in the combined sample using a model that included age, sex, diagnosis, and a FSIQ-by-diagnosis interaction. The interaction identified where in the brain group differences varied with FSIQ. In follow-up, we assessed effects of FSIQ on metabolites in ASD alone and TD alone using a model that included age and sex. Moreover, current use of any psychotropic medication (binary yes/no) was added to the model for all analyses that included ASD participants. All such analyses were repeated excluding ASD participants taking medication (for findings, see Supplemental Results). Findings are reported only for cases that were significant both when covarying for medication and when excluding medicated participants.

RESULTS

Effects of Diagnosis and Symptoms

Various metabolites levels (Figures 2, S1A, S2A) were lower ($p < 0.001–0.02$) in ASD in bilateral anterior cingulate cortex (ACC; NAA, Cho), middle cingulate cortex (MCC; NAA, Cr, Cho) and left white matter (NAA), middle temporal gyrus (MTG; NAA, Cr, Cho), inferior frontal cortex (IFC; NAA), and insula (NAA). Metabolites were higher ($p < 0.001–0.02$; Figures 2, S1A, S2A) in ASD *vs.* TD in bilateral posterior cingulate cortex (PCC; NAA, Glx) and mesial temporal lobe (MTL; Glx, Cr) and right internal capsule (IC; Glx, Cr, Cho).

Within ASD, multiple metabolites correlated inversely ($p < 0.001–0.02$) with *ADOS Total* score (Figures 2, S1B, S2B) bilaterally in several white-matter tracts (NAA, Glx, Cr, Cho), left precuneus (NAA, Glx, Cr) and right IFC (NAA, Cr, Cho). Multiple metabolites correlated positively with *SRS Total* score (Figures 2, S1C, S2C) in bilateral centrum semiovale, PCC and MCC (all $p = 0.001$; NAA, Glx, Cr, Cho) and in left caudate ($p = 0.02$; NAA, Glx). Glx, Cr, and Cho correlated inversely ($p < 0.001–0.02$) with the *ADOS Social Affect* subscore in white matter (Figures 3, S3). Several SRS subscores (Figures 3, S3–S7) correlated positively ($p < 0.001–0.02$) with metabolites in numerous regions. These included the *SRS Social Awareness* subscore (Figures 3, S4) in bilateral white matter, PCC, MCC (NAA, Glx, Cr, Cho) and precuneus (NAA, Cr, Cho) and right MTL (NAA, Glx), IFC (NAA, Glx, Cr), central opercular cortex (Cr, Cho), planum temporale (Cr, Cho) and ventral pallidum (NAA, Cr, Cho); the *SRS Social Cognition* subscore (Figures 3, S5) in bilateral white matter, PCC, MCC, precuneus (NAA, Glx, Cr, Cho), MTL (Cr, Cho), lenticular nucleus (Cr, Cho), ventral pallidum (Glx, Cho), right IFC (Cr, Cho), and planum temporale (Cr, Cho); the *SRS Social Communication* subscore (Figures 3, S6) in bilateral centrum semiovale, PCC, and precuneus (NAA, Glx, Cr, Cho); and the *SRS Restricted Behavior* subscore (Figures 3, S7) in bilateral white matter, PCC (NAA, Glx, Cr, Cho), MCC (Glx, Cr, Cho), and precuneus (Cr, Cho).

Age Effects

Bilateral positive age-by-diagnosis interactions were seen for metabolites in PCC (NAA, Cr), MCC (Cr), precuneus (NAA, Cr), and left MTG (NAA, Glx; Figures 4, S8A, S9A; $p = 0.001$). Each of these interactions derived from stronger inverse correlations of age with concentration in TD than in ASD (Figures 4, S8BC, S9BC). Right-sided negative interactions were seen in IC, insula, and MTL (NAA, Glx, Cr, Cho; Figures S8A, S9A; $p = 0.001$, except MTL $p = 0.02$) that derived from steeper inverse correlations of age with metabolite levels in ASD (Figures S9BC, S10BC).

Sex Effects

We detected a bilateral sex-by-diagnosis interaction in posterior thalamic radiations and a left-sided interaction in centrum semiovale (both $p = 0.001$, strongest for Glx and NAA) (Figures 4, S10–S11). In some regions, NAA and Glx were lower in males than females in TD, but higher in males than females in ASD. In other regions, ASD females had lower NAA and Glx, on a par with TD males, removing the normal pattern of lower metabolites in

males leading to the significant interaction. Lower metabolite levels were detected in male ASD compared to male TD (Figure S12) participants ($p < 0.0001–0.02$) in bilateral anterior corona radiata (ACR) and other white matter (NAA); bilateral ACC (NAA, Cr, Cho) and MCC (NAA, Cr, Cho); and left insula, MTG, and MTL (NAA, Cr, Cho). Higher levels ($p = 0.0001$) were present in ASD in left superior corona radiata (SCR; NAA), right SCR (Cr) and lenticular nucleus (Glx, Cr).

FSIQ Effects

FSIQ-by-diagnosis interactions ($p < 0.001–0.02$; Figures 5, S13–S14) were observed for metabolites bilaterally in white matter (NAA, Glx, Cr, Cho) and MCC (NAA, Cr), PCC (NAA, Glx, Cr), precuneus (NAA, Cr, Cho), insula (NAA, Glx, Cr, Cho), IFC (NAA, Glx, Cr, Cho), superior temporal cortex (STC; NAA, Glx, Cr, Cho), ventral pallidum (Cr), and thalamus (NAA). The interactions derived from lower metabolite levels with decreasing FSIQ in ASD, but either weak positive or inverse correlations of metabolites with FSIQ in TD.

DISCUSSION

This MRS study of ASD featured near whole-brain high-resolution coverage at high-field accounting for voxel-tissue composition, psychotropic medications, and multiple comparisons. The ASD and age-and sex-matched TD samples were larger than in most MRS studies and permitted evaluation of effects of diagnosis and symptom domains, and of age, sex, and IQ, on metabolites. Major findings were: 1) ASD was associated with below-TD NAA in white matter and perisylvian cortex, levels of all metabolites declining with symptom severity (ADOS Total Score and Social Affect subscore), and above-TD NAA and Glx in PCC increasing (along with Cr and Cho) with severity (SRS Total Score and subscores); 2) In certain brain regions (PCC, MCC, precuneus, MTG) NAA, Glx, or Cr decreased more slowly with age in ASD than in TD, and in a few regions (IC, insula, MTL) all metabolites decreased more rapidly; 3) Sex-differences in NAA and Glx were attenuated or reversed in ASD relative to TD, and male ASD compared to male TD participants had lower NAA, Cr, and Cho in multiple white-matter tracts; and 4) In numerous white-matter tracts and cortices, lower NAA, Glx, Cr, and Cho were associated with lower FSIQ in ASD, whereas lower levels of these metabolites were associated mostly with increasing FSIQ in TD. These findings underscore the need to account for sample heterogeneity in studies of ASD, but also indicate that heterogeneity in ASD has discrete underlying neurobiological determinants. Support is afforded for multiple theories of ASD as indicated below.

Effects of ASD Diagnosis and Symptoms

Metabolites (NAA, Cr, Cho) were lower in ASD than in TD and declined with increasing ADOS severity (NAA, Glx, Cr, Cho; Figures 2, S1B) in white matter and perisylvian cortex (IFC, insula). Few ASD MRS studies sampled IFC or insula (10–12), but other imaging modalities have implicated these regions in ASD (13–20), proposing deficits in the "mirror neuron system", theory of mind, or social brain. One small study (11) of adult ASD found elevated Glx in auditory cortex, while we found no significant effects on Glx there. The shorter-TE and targeted sampling of auditory cortex in (11) may have facilitated their

detection of this effect. Several MRS studies of white matter in ASD reported lower NAA (10,21–22), Glx (23), or Cr (10). Consistent with these findings are MRI (24–25) and DTI (26) reports of widespread white-matter abnormalities and postmortem axonal pathology (fewer long and more short axons, thinner myelin)(27–28) in ASD, perhaps representing compromised axonal or oligodendroglial integrity and impaired neurotransmission. Axonal pathology and white-matter abnormalities have been cited to support theories that ASD symptoms derive from cortico-cortical underconnectivity and compensatory local overconnectivity (29).

In aMCC, NAA, Cr, and Cho were lower in ASD than in TD (Figs. S1A,S2A) while NAA, Glx, Cr, and Cho correlated positively with SRS Total Score (S1C,S2C) and Social Cognition subscore (S5A,S5B) in pMCC. This may appear contradictory but is not necessarily so. First, the findings are in different, if adjacent, cingulate subregions (aMCC, pMCC). Second, even if in the same subregion, the reductions in metabolite levels could represent symptom-lowering compensatory responses. This principle applies generally where a between-group difference is accompanied by a within-patient-group symptom correlation of opposite sign.

NAA and Glx were elevated in PCC in ASD and higher levels of all four metabolites in PCC were associated with more severe symptoms (SRS; Figures 2, S1). The PCC (and precuneus) are underexplored with MRS in ASD (30), but abnormalities have been reported in pathology (abnormal cytoarchitecture)(31) and in other MR modalities (13–14,32). The PCC lies in the "default mode network" and "social brain" (33), and is linked to mental operations impaired in ASD, including theory of mind (34), internally directed attention (35), body ownership (36), and self-localization and performance monitoring (37).

Additional regional ASD effects without significant symptom correlates included reduced levels of all four metabolites in ACC and MTG (Figures S2A, S11A) and elevated Glx and Cr in MTL (hippocampus, amygdala, rostral lingual gyrus). ACC abnormalities are frequently reported in neuroimaging (20–21,32,38–42) and postmortem studies (pachygyria, dysplasia, heteropia, and small, closely packed neurons)(43–44). The ACC subserves social and executive functions impaired by ASD (45–46). The lateral temporal lobe, including MTG, has been less explored with MRS in ASD (15), but abnormalities are reported in other neuroimaging (14,20,47) and postmortem studies (smaller, more numerous mini-columns) (43). The MTG and STG are thought to be sites of ASD impairments in face processing (48), and theory of mind (49). MTL abnormalities, reported in metabolite (50–52) and volumetric (53) studies, are consistent with amygdalar and hippocampal theories of ASD (54).

In several regions, metabolites correlated with symptom severity in the absence of ASD main effects. Levels in white-matter of the IC (NAA, Glx), SLF (Glx, Cr), and PCR (Glx, Cr, Cho) correlated inversely with ADOS symptoms, indicating that widespread white-matter metabolite reductions accompany more severe illness. Metabolite levels correlated positively with SRS in CSO (NAA, Cr, Cho), MCC (NAA, Glx, Cr, Cho), and caudate (NAA). MCC abnormalities have been reported in several prior MRS studies (10,30,55–56) and a postmortem study (smaller, more numerous neurons)(57) and this region is a possible

locus of social and cognitive impairments in ASD (45). Abnormal caudate metabolites (10,21), volumes (58–59), and cellularity (low interneuron density)(60–61) have been reported in ASD.

Age Effects

Positive age-by-diagnosis interactions were found in PCC (NAA, Cr), MCC (Cr), precuneus (NAA, Glx, Cr), and MTG (NAA) based on inverse correlations with age in TD controls, but no correlation in ASD. Inverse correlations with age were less significant and less spatially extensive in ASD than TD (Supplemental Figure S8A–D). In a few regions (IC, insula, MTL) steeper inverse correlations of all four metabolites with age were seen in ASD. Age interactions involving metabolites have occasionally been reported in ASD (52), but the topic is underexplored. MRI has revealed aberrant growth patterns for brain structures in ASD (62–63), suggesting anomalous developmental trajectories for regional neurometabolites, especially in cortex, for ASD as well.

Sex Effects

For the overall sample, in several regions TD had lower levels of one or more metabolites for males than females, while ASD had higher levels for males. In some regions, ASD females had lower metabolites comparable to those of TD males, violating the TD males lower than female pattern. This suggests that the ASD females were relatively akin to males in their spatial pattern of metabolite levels. We are unaware of prior reports of MRS sex differences in ASD. ASD affects males more frequently than females (1) leading to an "extreme male brain theory" of ASD (64). The diminished male-female metabolite differences presently seen modestly support this notion, but in most regions male-female metabolite differences were similar in ASD and TD, and effects for ASD *vs.* TD males largely resembled effects for the overall sample. Larger metabolite studies of females with ASD are needed to test this theory more rigorously.

FSIQ Effects

FSIQ moderated effects of diagnosis on metabolite levels in numerous brain regions (Figure 5). Although there was much overlap in FSIQ between the ASD and TD samples, positive correlations in ASD indicated that one or more metabolite levels declined with decreasing FSIQ in white (SCR, ACR, PCR, CC, SLF) and gray matter (MCC, PCC, VP, Th, Ins, STC), whereas correlations with FSIQ were weaker or opposite in TD. These findings suggest that the general reductions in metabolite levels we detected as a main effect of ASD are larger in ASD participants with lower IQs. Metabolite correlates of IQ have been reported in some ASD studies (30,41,50), but most studies have excluded low-functioning participants, whom we included intentionally to assess IQ effects and to improve generalizability of findings. The regional distribution of FSIQ effects in ASD corresponded closely to the distribution of SRS severity correlates (Figures 2–3, 5) but were statistically independent of them, suggesting that the same metabolic signature contributes to both lower IQ and more severe symptoms, which together are often considered "lower functioning" in ASD.

Commonality of Effects Across Metabolites

Most effects involved multiple metabolites, in the same direction and anatomically overlapping. This has various possible explanations. Jointly depressed metabolites in ASD could represent reduced cellularity in those regions, either from reduced proliferation or differentiation of cells early in development or from altered plasticity later in development, consistent with postmortem studies (43–44,57) reporting smaller neurons in ASD. Second, disturbances in cell-energy metabolism in ASD could account for the commonality of observed effects. NAA levels correlate with glucose metabolic rate (65–66). Since NAA is synthesized in neuronal mitochondria (67) from the glycolysis product acetyl-CoA, NAA is thought to store substrate for longer-term energy expenditure (68). Moreover, NAA is catabolized by oligodendrocytes (69) to support myelin synthesis (68). Lower NAA in ASD therefore may indicate reduced long-term energy storage, from lower brain energetics or greater oligodendrocyte catabolism. Glutamatergic neurotransmission is a cell-energy sink, while glutamate and glutamine are Krebs cycle reactants and glutamine plays a role in recycling of glutamate. Lower Glx may reflect reduced neurotransmitter activity and, hence, reduced energetic demands. MRS Cr represents the creatine-phosphocreatine ATP buffer for short-term energy (70). Lower Cr may indicate reduced short-term energy storage, perhaps deriving from reduced glutamatergic neurotransmission. Choline-compounds are mostly bound in membrane phospholipids and therefore are invisible to ^{1}H MRS (71). Cell membranes, however, undergo continuous remodeling and turnover, hydrolyzing phospholipids into water-soluble choline, phosphocholine, and glycerophosphocholine that MRS quantifies. Low MRS Cho could therefore reflect reduced membrane turnover (72). Low Cho could further imply that carbon substrate is being consumed to meet cell-energy demands, rather than built into cell membranes. Thus, any process that alters neuroenergetics will likely influence multiple MRS resonances. In particular, mitochondrial dysfunction disturbs multiple MRS metabolites (73); we previously reported MRS evidence for mitochondrial dysfunction in this sample (31). Finally, inflammatory processes affect multiple metabolites (74), and ASD may represent a neuroinflammatory condition (75).

Limitations

Medication was used by 26 of 78 ASD participants. Recruiting medication-free ASD samples is difficult, and curtails generalizability of findings. Moreover, we only reported effects that were significant both when covarying for medication and when excluding medicated participants. Participants varied widely in age, by design, as it allowed us to assess age effects directly. Mean IQ was slightly lower in the ASD than TD sample. After removing 1 ASD participant with FSIQ = 52 this difference was no longer significant, but metabolite findings were not altered. MPCSI was acquired at high-field, but long-TE, thus segregating Glu from Glx was not possible. Although some might question reporting Glx at all under these conditions, our Glx data survived the same rigorous quality control as the other metabolites. Long-TE acquisition (here TE144) is more stable than short-TE for MPCSI. Glx has been previously measured successfully at long-TE (76–78), and quantitation of Glx at TE144 has been deemed methodologically acceptable at 3 T (79). Nonetheless, TE144 is not optimal for Glx, so results merit replication at short-TE. Due to the challenges of measuring T2-values, metabolites levels were not corrected for T2-relaxation, hence, abnormal T2 in ASD could underlie presently observed metabolite effects

(10). These weaknesses are counterbalanced by strengths of our study, including large sample, wide coverage, high spatial-resolution, accounting for tissue-composition, and assessing effects of age, sex, and IQ. Overall findings help parse the neurometabolic signature for ASD and cohere with ASD theories (18,24–25,33–34,54,64,75).

Supplementary Material

Refer to Web version on PubMed Central for supplementary material.

ACKNOWLEDGMENTS AND DISCLOSURES

This study was supported by NIMH grant R01 MH089582 and funding from Children's Hospital Los Angeles and the University of Southern California. The research was made possible by the provision of data by New York State Psychiatric Institute and Columbia University. We thank Dr. Zhengchao Dong for contributions to acquisition and post-processing. We are grateful to Zachary Toth, Carlo Nati, and Dr. Molly Algermissen for their technical assistance. Martina Rodie was supported by the St Andrew's Society/Glasgow Children's Hospital Charity Visiting Scholarship. The authors report no biomedical financial interests or potential conflicts of interest.

REFERENCES

1. Center For Disease Control (CDC) (2009): Prevalence of autism spectrum disorders-Autism and Developmental Disabilities Monitoring Network, United States, 2006. MMWR Surveill Summ 58(SS10): 1–20.
2. Levitt JG, O'Neill J, Alger JR (2013): Magnetic resonance spectroscopy studies of autistic spectrum disorders (ASD) In: Blüml S, Panigrahy A, editors. MR Spectroscopy of Pediatric Brain Disorders. New York: Springer, pp 213–228.
3. Ford TC, Crewther DP (2016): A comprehensive review of the 1H-MRS metabolite spectrum in Autism Spectrum Disorder. Fron Molec Neurosci 9(14): 1–27.
4. Goh S, Dong ZC, Zhang YD, DiMauro S, Peterson BS (2014): Mitochondrial dysfunction as a neurobiological subtype of autism spectrum disorder: Evidence from brain imaging. JAMA Psychiatry 71(6): 665–671. [PubMed: 24718932]
5. Lord C, Rutter M, Le Couteur A (1994): Autism Diagnostic Interview: a revised version of a diagnostic interview for caregivers of individuals with possible pervasive developmental disorders. J Autism Dev Disord 24(5): 659–685. [PubMed: 7814313]
6. Lord C, Risi S, Lambrecht L, Cook EH Jr, Leventhal BL DiLavore PC, Pickles A, Rutter M (2000): The Autism Diagnostic Observation Schedule-Generic: a standard measure of social and communication deficits associated with the spectrum of autism. J Autism Dev Disord 30(3): 205–223. [PubMed: 11055457]
7. Constantino JN (2002): The Social Responsiveness Scale. Los Angeles: Western Psychological Services.
8. Hao X, Xu D, Bansal R, Dong Z, Liu J, Wang Z, Kangarlu A, Liu F, Duan Y, Shova S, Gerber AJ, Peterson BS (2013): Multimodal magnetic resonance imaging: The coordinated use of multiple, mutually informative probes to understand brain structure and function. Hum Brain Mapp 34(2): 253–271. [PubMed: 22076792]
9. O'Neill J, Dong Z, Bansal R, Ivanov I, Hao X, Desai J, Pozzi E, Peterson BS (2016). Proton chemical shift imaging of the brain in pediatric and adult developmental stuttering. JAMA Psychiatry 74(1): 85–94.
10. Friedman SD, Shaw DW, Artru AA, Richards TL, Gardner J, Dawson G, Posse S, Dager SR. (2003): Regional brain chemical alterations in young children with autism spectrum disorder. Neurology 60(1): 100–107. [PubMed: 12525726]
11. Brown MS, Singel D, Hepburn S, Rojas DC (2013): Increased glutamate concentration in the auditory cortex of persons with autism and first-degree relatives: A 1H-MRS study. Autism Res 6(1): 1–10. [PubMed: 23166003]

12. Rojas DC, Singel D, Steinmetz S, Hepburn S, Brown MS (2014): Decreased left perisylvian GABA concentration in children with autism and unaffected siblings. NeuroImage 86: 28–34. [PubMed: 23370056]
13. Bonilha L, Cendes F, Rorden C, Eckert M, Dalgalarrondo P, Li LM, Steiner CE (2008): Gray and white matter imbalance-Typical structural abnormality underlying classic autism? Brain & Devel 30: 396–401.
14. Jann K, Hernandez LM, Beck-Pancer D, McCarron R, Smith RX, Dapretto M, Wang DJJ (2015): Altered resting perfusion and functional connectivity of default mode network in youth with autism spectrum disorder. Brain Behav 5(9):e00358. [PubMed: 26445698]
15. Kosaka H, Omori M, Munesue T, Ishitobi M, Matsumura Y, Takahashi T, Narita K, Murata T, Saito DN, Uchiyama H, Morita T, Kikuchi M, Mizukami K, Okazaza H, Sadato N, Wada Y (2010): Smaller insula and inferior frontal volumes in young adults with pervasive developmental disorders. NeuroImage 50(4): 1357–1363. [PubMed: 20123027]
16. Cauda F, Geda E, Sacco K, D'Agata F, Duca S, Geminiani G, Keller R (2011): Grey matter abnormality in autism spectrum disorder: an activation likelihood estimation meta-analysis study. J Neurol Neurosurg Psychiatry 82: 1304–1313. [PubMed: 21693631]
17. Libero LE, DeRamus TP, Lahti AC, Deshpande G, Kana RK (2015): Multimodal neuroimaging based classification of autism spectrum disorder using anatomical, neurochemical, and white matter correlates. Cortex 66: 46–59. [PubMed: 25797658]
18. Dapretto M, Davies MS, Pfeifer JH, Scott AA, Sigman M, Bookheimer SY, Iacoboni M (2006): Understanding emotions in others: mirror neuron dysfunction in children with autism spectrum disorders. Nat Neurosci 9(1): 28–30. [PubMed: 16327784]
19. Kleinhans NM, Schweinsburg BC, Cohen DN, Müller R-A, Courchesne E (2007): N-acetyl aspartate in autism spectrum disorders: Regional effects and relationship to fMRI activation. Brain Res 1162: 85–97. [PubMed: 17612510]
20. Di Martino A, Shehzad Z, Kelley C, Roy AK, Gee DG, Uddin LQ, Gotimer K, Klein DF, Castellanos FX, Milham MP (2009): Relationship between cingulo-insular functional connectivity and autistic traits in neurotypical adults. Am J Psychiatry 166: 891–899. [PubMed: 19605539]
21. Levitt JG, O'Neill J, Blanton RE, Smalley S, Fadale D, McCracken JT, Guthrie D, Toga AW, Alger JR (2003): Proton magnetic resonance spectroscopic imaging of the brain in childhood autism. Biol Psychiatry 54(12): 1355–1366. [PubMed: 14675799]
22. Hardan AY, Fung LK, Frazier T, Berqusit SW, Minshew NJ, Keshavan MS, Stanley JA (2016): A proton spectroscopy study of white matter in children with autism. Prog Neuro-Psychopharm Biol Psychiatry 66: 48–53.
23. Kubas B, Kulak W, Sobaniec W, Tarasow E, Lebkowska U, Walecki J (2012): Metabolite alterations in autistic children: a 1H MR spectroscopy study. Adv Med Sciences 57(1): 152–156.
24. Courchesne E (2004): Brain development in autism: early overgrowth followed by premature arrest of growth. Ment Retard Dev Disabil Res Rev 10: 106–111. [PubMed: 15362165]
25. Herbert MR, Ziegler DA, Makris N, Filipek P, Kemper TL, Normandin JJ, Sanders HA, Kennedy DN, Cavinees VS Jr (2004): Localization of white matter volume increase in autism and developmental language disorder. Ann Neurol 55: 530–540. [PubMed: 15048892]
26. Travers BG, Adluru N, Ennis C, Tromp DPM, Destiche D, Doran S, Bigler ED, Lange N, Lainhart JE, Alexander AL (2012): Diffusion tensor imaging in autism spectrum disorder: a review. Autism Res 5: 289–313. [PubMed: 22786754]
27. Courchesne E, Pierce K, Schumann CM, Redcay E, Buckwalter JA, Kennedy DP, Morgan J (2007): Mapping early brain development in autism. Neuron 56(2): 399–413. [PubMed: 17964254]
28. Zikopoulos B, Barbas H (2010): Changes in prefrontal axons may disrupt the network in autism. J Neurosci 30(44): 14595–14609. [PubMed: 21048117]
29. Courchesne E, Pierce K (2005): Brain overgrowth in autism during a critical time in development: implications for frontal pyramidal neuron and interneuron development and connectivity. Int J Dev Neurosci 23: 153–170. [PubMed: 15749242]
30. Libero LE, Reid MA, White DM, Salibi N, Lahti AC, Kana RK (2016): Biochemistry of the cingulate cortex in autism: An MR spectroscopy study. Autism Res 9:643–657. [PubMed: 26526126]

31. Oblak AL, Rosene DL, Kemper TL, Bauman ML, Blatt GJ (2011): Altered posterior cingulate cortical cyctoarchitecture, but normal density of neurons and interneurons in the posterior cingulate cortex and fusiform gyrus in autism. Autism Res; 4: 200–211. [PubMed: 21360830]
32. Kennedy DP, Redcay E, Courchesne E (2006): Failing to deactivate: Resting functional abnormalities in autism. Proc Natl Acad Sci USA 103(21): 8275–8280. [PubMed: 16702548]
33. Adolphs R (2009): The social brain: neural basis of social knowledge. Ann Rev Psych 60: 693–716.
34. Fletcher PC, Happe F, Frith U, Baker SC, Dolan RJ, Frackowiak RS (1995): Other minds in the brain: a functional imaging study of "theory of mind" in story comprehension. Cogn 57: 109–128.
35. Leech R, Sharp DJ (2014): The role of the posterior cingulate cortex in cognition and disease. Brain 137(Pt 1): 12–32. [PubMed: 23869106]
36. Guterstam A, Björnsdotter M, Gentile G, Ehrsson HH (2015): Posterior cingulate cortex integrates the senses of self-location and body ownership. Curr Biol 25(11): 1416–1425. [PubMed: 25936550]
37. Heilbronner SR, Platt ML (2013): Causal evidence of performance monitoring by neurons in posterior cingulate cortex during learning. Neuron 80(6): 1384–1391. [PubMed: 24360542]
38. Bejjani A, O'Neill J, Kim JA, Frew AJ, Yee VW, Ly R, Kitchen C, Salamon N, McCracken JT, Toga AW, Alger JR, Levitt JG (2012): Elevated glutamatergic compounds in pregenual anterior cingulate in pediatric autism spectrum disorder demonstrated by 1H MRS and 1H MRSI. PLos One 7(7): e38786. [PubMed: 22848344]
39. Joshi G, Biederman J, Wozniak J, Goldin RL, Crowley D, Furtak S, Lukas SE, Gönenç A (2013): Magnetic resonance spectroscopy study of the glutamatergic system in adolescent males with high-functioning autistic disorder: a pilot study at 4T. Eur Arch Psychiatry Clin Neurosci 263(5): 379–384. [PubMed: 22986449]
40. Bernardi S, Anagnostou E, Shen J, Kolevzon A, Buxbaum JD, Hollander E, Hof PR, Fan J (2011): In vivo 1H-magnetic resonance spectroscopy study of the attentional networks in autism. Brain Res 1380: 198–205. [PubMed: 21185269]
41. Cochran DM, Sikoglu EM, Hodge SM, Edden RAE, Foley A, Kennedy DN, Moore CM, Frazier JA (2015): Relationship among glutamine, γ-aminobutyric acid, and social cognition In autism spectrum disorders. J Child Adol Psychopharm 25(4): 314–322.
42. Thakker KN, Polli FE, Joseph RM, Tuch DS, Hadjikhani N, Barton JJS, Manoach DS (2008) Response monitoring, repetitive behaviour and anterior cingulate abnormalities in autism spectrum disorders (ASD). Brain 131: 2464–2478. [PubMed: 18550622]
43. Casanova MF, Buxhoeveden DP, Switala AE, Roy E (2002): Minicolumnar pathology in autism. Neurology 58: 428–432. [PubMed: 11839843]
44. Simms ML, Kemper TL, Timbie CM, Bauman ML, Blatt GJ (2009): The anterior cingulate cortex in autism: heterogeneity of qualitative and quantitative cytoarchitectonic features suggests possible subgroups. Acta Neuropathol 118: 673–684. [PubMed: 19590881]
45. Mundy P (2003): Annotation: The neural basis of social impairments in autism: The role of the dorsal medial-frontal cortex and anterior cingulate system. J Child Psychol Psychiatry 44: 793–809. [PubMed: 12959489]
46. Amodio DM, Frith CD (2006): Meeting of minds: the medial frontal cortex and social cognition. Nature Rev Neurosci 7: 268–277. [PubMed: 16552413]
47. Uddin LQ, Supekar K, Lynch CJ, Khouzam A, Phillips J, Feinstein C, Ryali S, Menon V (2013): Salience network–based classification and prediction of symptom severity in children with autism. JAMA Psychiatry 70(8): 869–879. [PubMed: 23803651]
48. Puce A, Allison T, Bentin S, Gore JC, McCarthy G (1998): Temporal cortex activation in humans viewing eye and mouth movements. J Neurosci 18: 2188–2199. [PubMed: 9482803]
49. Baron-Cohen S, Ring HA, Wheelwright S, Bullmore ET, Brammer MJ, Simmons A, Williams SC (1999): Social intelligence in the normal and autistic brain: an fMRI study. Eur J Neurosci 11(6): 1891–1898. [PubMed: 10336657]
50. Mori K, Toda Y, Ito H, Mori T, Goji A, Fujii E, Miyazaki M, Harada M, Kagami S (2013): A proton magnetic resonance spectroscopic study in autism spectrum disorders: Amygdala and orbito-frontal cortex. Brain & Devel 35: 139–145.

51. Page LA, Daly E, Schmitz N, Simmons A, Toal F, Deeley Q, Ambery F, McAlonan GM, Murphy KC, Murphy DGM (2006): In vivo 1H-magnetic resonance spectroscopy study of amygdala-hippocampal and parietal regions in autism. Am J Psychiatry 163: 2189–2192. [PubMed: 17151175]
52. O'Brien FM, Page L, O'Gorman RL, Bolton P, Sharma A, Baird G, Daly E, Hallahan B, Conroy RM, Foy C, Curran S, Robertson D, Murphy KC, Murphy DGM (2010): Maturation of limbic regions in Asperger syndrome: A preliminary study using proton magnetic resonance spectroscopy and structural magnetic resonance imaging. Psychiatry Res: Neuroimaging 184: 77–85. [PubMed: 20952166]
53. Sparks BF, Friedman SD, Shaw DW, Aylward EH, Echelard D, Artru AA, Dager SR (2002): Brain structural abnormalities in young children with autism spectrum disorder. Neurology 59(2): 184–192. [PubMed: 12136055]
54. Baron-Cohen S, Ring HA, Bullmore ET, Wheelwright S, Ashwin C, Williams SCR (2000): The amygdala theory of autism. Neurosci Biobehav Res 24: 355–364.
55. Vasconcelos MM, Rocha Brito A, Cortes Domingues R, Hygino da Cruz LC Jr, Gasparetto EL, Werner J, Sevalho Gonçalves JP (2008): Proton magnetic resonance spectroscopy in school-aged autistic children. J Neuroimaging 18: 288–295. [PubMed: 18304036]
56. Goji A, Ito H, Mori K, Harada M, Hisaoka S, Toda Y, Mori T, Abe Y, Miyazaki M, Kagami S (2017): Assessment of anterior cingulate cortex (ACC) and left cerebellar metabolism in Asperger's Syndrome with proton magnetic resonance spectroscopy (MRS). PLoS One 12(1): e0169288. [PubMed: 28060873]
57. Uppal N, Wicinski B, Buxbaum JD, Heinsen H, Schmitz C, Hof PR (2014): Neuropathology of the anterior midcingulate cortex in young children with autism. J Neuropathol Exp Neurol 73(9): 891–902. [PubMed: 25101703]
58. Voelbel GT, Bates ME, Buckman JF, Pandina G, Hendren RL (2006): Caudate nucleus volume and cognitive performance: Are they related in childhood psychopathology? Biol Psychiatry 60: 942–950. [PubMed: 16950212]
59. Langen M, Bos D, Noordermeer SDS, Nederveen H, van Engeland H, Durston S (2014): Changes in the development of striatum are involved in repetitive behavior in autism. Biol Psychiatry 76: 405–411. [PubMed: 24090791]
60. Wegiel J, Flory M, Kuchna I, Nowicki K, Ma SY, Imaki H, Wegiel J, Cohen IL, London E, Wisniewski T, Brown WT (2014): Stereological study of the neuronal number and volume of 38 brain subdivisions of subjects diagnosed with autism reveals significant alterations restricted to the striatum, amygdala and cerebellum. Acta Neuropathologica Comm 2: 141.
61. Adorjan I, Ahmed B, Feher V, Torso M, Krug K, Esiri M, Chance SA, Szele FR (2017): Calretinin interneuron density in the caudate nucleus is lower in autism spectrum disorder. Brain 140: 2028–2040. [PubMed: 29177493]
62. Courchesne E, Karns CM, Davis HR, Ziccardi R, Carper RA, Tigue ZD, Courchesne RY (2001): Unusual brain growth patterns in early life in patients with autistic disorder: An MRI study. Neurology 57(2): 245–254. [PubMed: 11468308]
63. Hua X, Thompson PM, Leow AD, Madsen SK, Caplan R, Alger JR, O'Neill J, Joshi K, Smalley SL, Toga AW, Levitt JG (2013): Brain growth rate abnormalities visualized in adolescents with autism. Hum Brain Mapping 34(2): 425–436.
64. Baron-Cohen S (2002): The extreme male brain theory of autism. Trends Cog Sci 6: 248–254.
65. O'Neill J, Eberling IL, Schuff N, Jagust W, Reed B, Soto G, Ezekiel F, Klein G, Weiner MW (2000): Method to correlate H-1 MRSI and (18)FDG-PET. Magn Reson Med 43(2): 244–250. [PubMed: 10680688]
66. Moreno A, Ross BD, Bluml S (2001): Direct determination of the N-acetyl-L-aspartate synthesis rate in the human brain by C-13 MRS and [1-C-13]glucose infusion. J Neurochem 77(1): 347–350. [PubMed: 11279290]
67. Wiame E, Tyteca D, Pierrot N, Collard F, Amyere M, Noel G, Desmedt J, Nassogne MC, Vikkula M, Octave JN, Vincent MF, Courtoy PJ, Boltshauser E, Van Schaftingen E (2010): Molecular identification of aspartate N-acetyltransferase and its mutation in hypoacetylaspartia. Biochem J 425: 127–136.

68. Ariyannur PS, Moffett JR, Manickam P, Pattabiraman N, Arun P, Nitta A, Nabeshima T, Madhavarao CN, Namboodiri AMA (2010): Methamphetamine-induced neuronal protein NAT8L is the NAA biosynthetic enzyme: Implications for specialized acetyl coenzyme A metabolism in the CNS. Brain Res 1335: 1–13. [PubMed: 20385109]
69. Moffett JR, Arun P, Ariyannur PS, Garbern JY, Jacobowitz DM, Namboodiri AMA (2011): Extensive aspartoacylase expression in the rat central nervous system. Glia 59(10): 1414–1434. [PubMed: 21598311]
70. Wallimann T, Tokarska-Schlattner M, Schlattner U (2011): The creatine kinase system and pleiotropic effects of creatine. Amino Acids 40(5): 1271–1296. [PubMed: 21448658]
71. Loffelholz K, Klein J, Koppen A (1993): Choline, a precursor of acetylcholine and phospholipids in the brain. Cholinergic Func Dysfunc 98: 197–200.
72. Poptani H, Gupta RK, Gupta K, Roy R, Pandey R, Jain VK, Chhabra DK (1995): Characterization of intracranial mass lesions with in-vivo proton MR spectroscopy. Am J Neuroradiol 16(8): 1593–1603. [PubMed: 7502961]
73. Stork C, Renshaw PF (2005): Mitochondrial dysfunction in bipolar disorder: evidence from magnetic resonance spectroscopy research. Molec Psychiatry 10: 900–919. [PubMed: 16027739]
74. Chang L, Munsaka SM, Kraft-Terry S, Ernst T (2013): Magnetic resonance spectroscopy to assess neuroInflammation and neuropathic pain. J Neuroimm Pharmacol 8: 576–593.
75. Masi A, Quintana DS, Glozier N, Lloyd AR, Hickie IB, Guastella AJ (2015): Cytokine aberrations in autism spectrum disorder: a systematic review and meta-analysis. Molec Psychiatry 20: 440–446. [PubMed: 24934179]
76. DeVito TJ, Drost DJ, Neufeld RWJ, Rajakumar N, Pavlosky W, Williamson P, Nicolson R (2007): Evidence for cortical dysfunction in autism: A proton magnetic resonance spectroscopic imaging study. Biol Psychiatry 61: 465–473. [PubMed: 17276747]
77. Khiat A, D'Amour M, Souchon F, Boulanger Y (2010): MRS study of the effects of minocycline on markers of neuronal and microglial integrity in ALS. Magn Reson Imaging 28:1456–1460. [PubMed: 20832222]
78. Maddock RJ, Buonocore MH, Miller AR, Yoon JH, Soosman SK, Unruh AM (2013): Abnormal activity-dependent brain lactate and glutamate+glutamine responses in panic disorder. Biol Psychiatry 73: 1111–1119. [PubMed: 23332354]
79. Hancu I (2009): Optimized glutamate detection at 3T. J Magn Reson Imaging 30:1155–1162. [PubMed: 19856449]

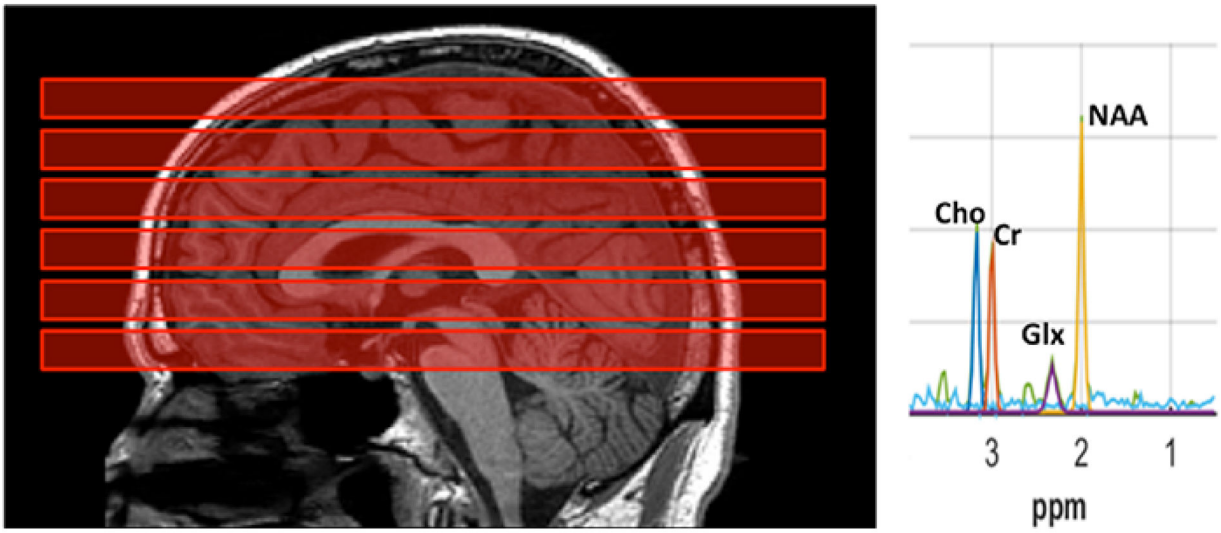

Figure 1.

Sagittal T1-weighted MRI of the brain (left) of a participant with autistic spectrum disorder (ASD) shows prescription of the 6 multiplanar chemical shift imaging (MPCSI; repetition-time [TR]/echo-time [TE]=2800/144 ms) slabs (red blocks), each parallel to the anterior commissure–posterior commissure (AC-PC) plane. Each slab was 10 mm thick with 2-mm interslice gap. One slab passed through the AC-PC, one was just inferior to it, and 4 slices were superior to the AC-PC. In-plane, nominal MPCSI voxel size was 10×10 mm^2. Lipid-suppression was achieved by 8 extracranial saturation bands (not shown). Typical MPCSI spectrum from an individual 10×10 mm^2 voxel (right) plotting radio-frequency signal intensity *vs.* chemical-shift in parts-per-million (ppm). Well-resolved resonances are seen for *N*-acetyl-compounds (NAA), glutamate+glutamine (Glx), creatine+phosphocreatine (Cr), and choline-compounds (Cho). Note narrow bandwidth, high signal-to-noise ratio (SNR), and flat baseline uncontaminated by extracranial lipids, macromolecules, or unsuppressed water.

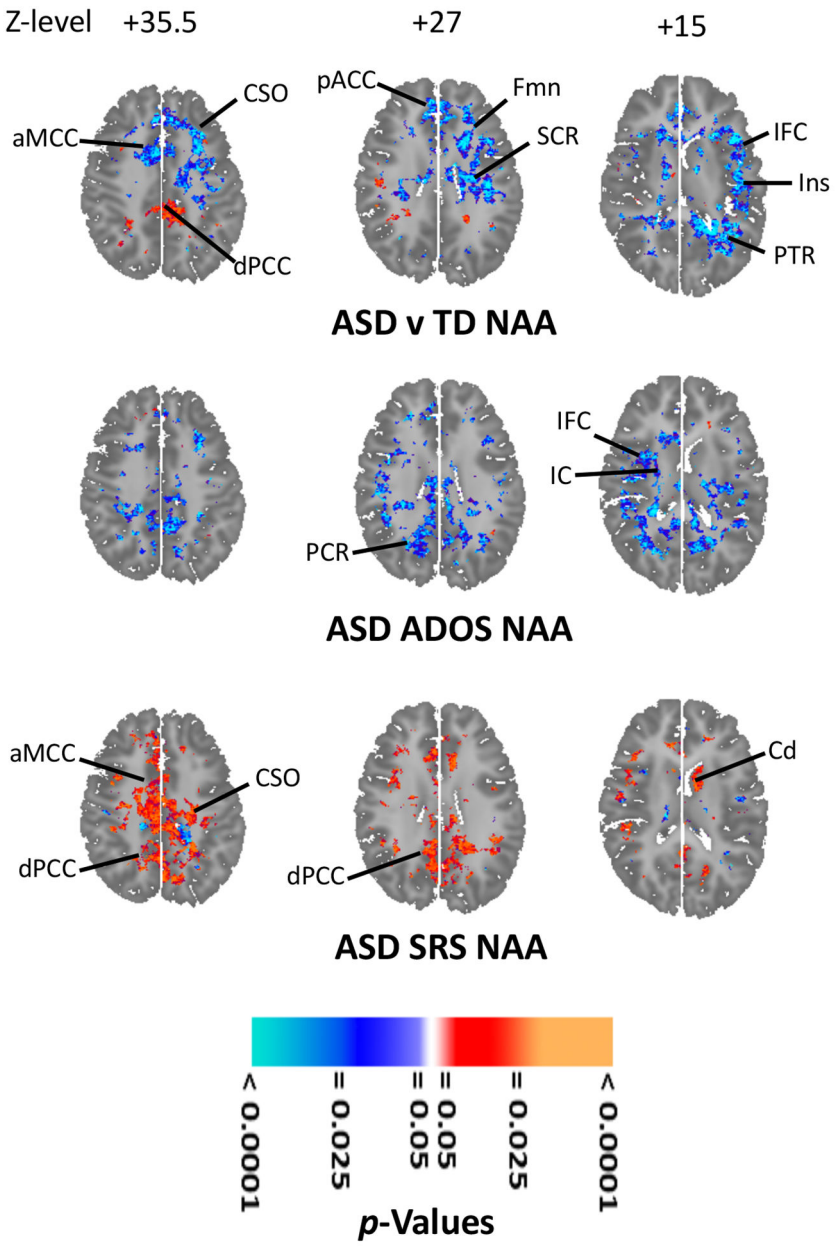

Figure 2.

Effects of autistic spectrum disorder (ASD) and its symptoms on *N*-acetyl-compounds (NAA) levels. Statistical parametric maps on axial brain template. NAA is higher (orange-red) for 68 ASD than for 93 typically developing (TD) participants in dorsal posterior cingulate cortex (dPCC)(left upper); NAA is lower (cyan-blue) in centrum semiovale (CSO), forceps minor (FMn), superior corona radiata (SCR), posterior thalamic radiations (PTR), anterior middle cingulate cortex (aMCC), pregenual anterior cingulate cortex (pACC), inferior frontal cortex (IFC) and insula (Ins). (Covariates: age, sex, FSIQ and use of any psychotropic medication.) NAA (left middle) correlated inversely (cyan-blue) with symptoms (Autism Diagnostic Observation Schedule—ADOS--Total Score) in posterior corona radiata (PCR), internal capsule (IC) and IFC. (Covariates: age, sex, medication; 68

ASD.) NAA (left lower) correlated positively (orange-red) with symptoms (Social Responsiveness Scale—SRS--Total Score) in CSO, aMCC, dPCC, and left caudate (Cd). (Covariates: age, sex, medication; 62 ASD.) All results corrected for multiple comparisons using false discovery rate. For further results including similar effects for other anatomic sections and other metabolites see Supplemental Results.

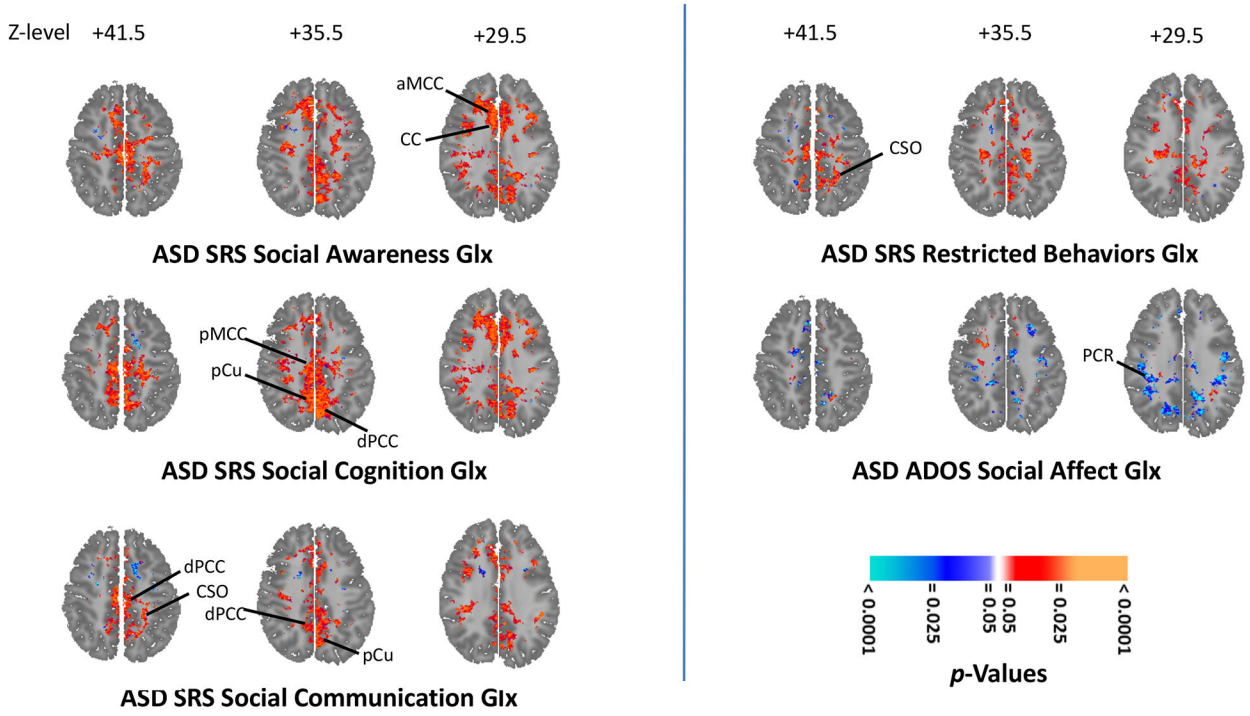

Figure 3.

Glutamatergic neuroanatomic profile of social symptoms in 62 participants with autistic spectrum disorder (ASD). Statistical parametric maps on selected axial brain sections show significance of correlations (orange-red for positive; cyan-blue for negative) of magnetic resonance spectroscopy levels of glutamate+glutamine (Glx) with scores on multiple subscales (left) of the Social Responsiveness Scale (SRS) reflecting different types of social symptoms in ASD. SRS Social Awareness symptoms (left upper) increase with increasing Glx in anterior middle cingulate cortex (aMCC) and corpus callosum (CC). SRS Social Cognition symptoms (left middle) increase with increasing Glx in posterior middle cingulate cortex (pMCC), precuneus (pCu), and dorsal posterior cingulate cortex (dPCC). SRS Social Communication symptoms (left lower) increase with increasing Glx in dPCC, centrum semiovale (CSO), and pCu. For comparison (right upper), correlations of (non-social) SRS Restricted Behaviors symptoms with Glx. For further comparison (right middle), correlations of Glx with social symptoms of yet another type, captured by a different instrument, the Autism Diagnostic Observation Schedule (ADOS) Social Affect subscale. These symptoms decrease with increasing Glx in the posterior corona radiata (PCR). (For correlations elsewhere in the brain and with other metabolites see Supplemental Figures S3–SS7.) All analyses covary for age, sex, FSIQ, and use of any psychotropic medication and are corrected for multiple comparisons using false discovery rate (FDR).

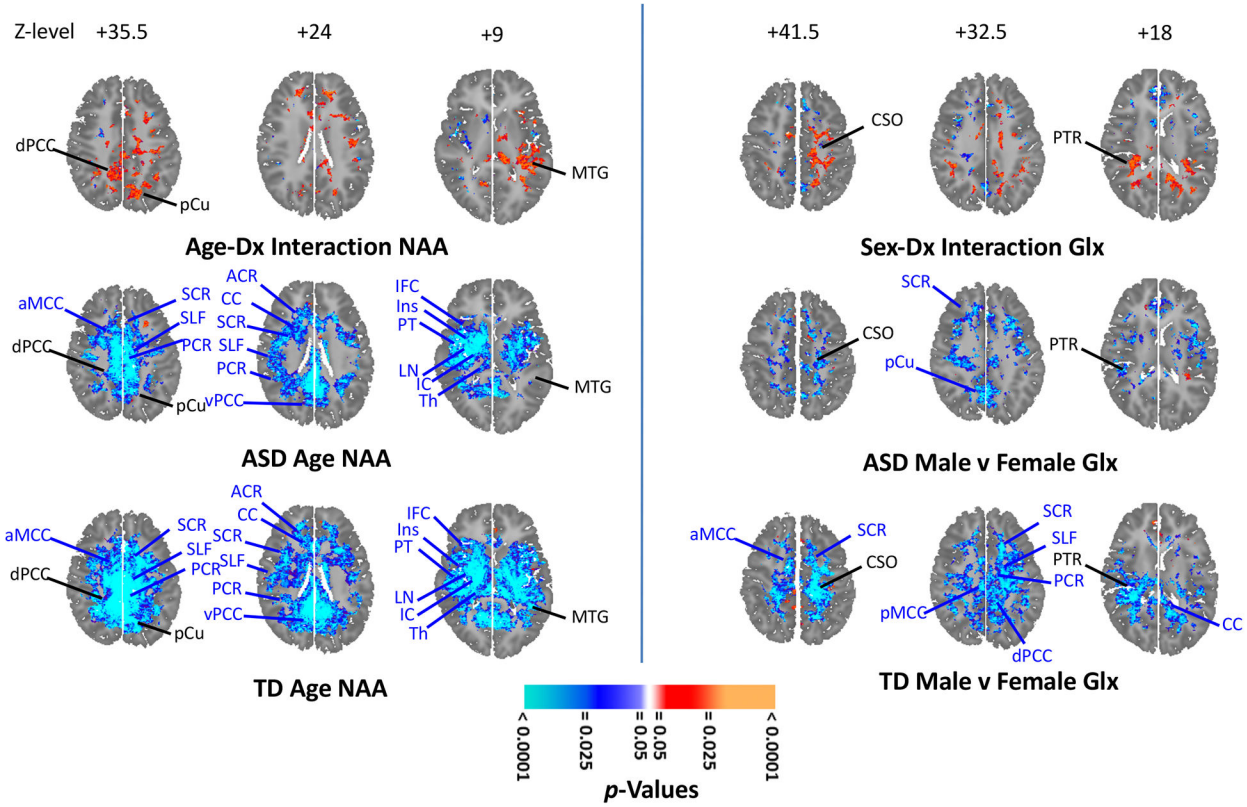

Figure 4.

Statistical parametric maps on selected axial brain sections show effects of age (left) on *N*-acetyl-compounds (NAA) and effects of sex (right) on glutamate+glutamine (Glx) in autistic spectrum disorder (ASD) and typically developing (TD) participants (all analyses false discovery rate–FDR--corrected). Age-by-diagnosis interactions (left upper; orange-red positive; cyan-blue negative) for NAA covarying for sex, diagnosis, and use of any psychotropic medication. Interactions were seen in dorsal posterior cingulate cortex (dPCC), precuneus (pCu), and middle temporal gyrus (MTG). Correlations (left middle; orange-red positive; cyan-blue negative) of NAA with age in 78 ASD participants, covarying for sex and use of any psychotropic medication. NAA decreased with age at multiple sites, including anterior middle cingulate cortex (aMCC), superior corona radiata (SCR), superior longitudinal fasciculus (SLF), posterior corona radiata (PCR), anterior corona radiata (ACR), corpus callosum (CC), ventral posterior cingulate cortex (vPCC), inferior frontal cortex (IFC), insula (Ins), planum temporale (PT), lenticular nucleus (LN), internal capsule (IC), and thalamus (Th). Significant interaction sites in black. Correlations of NAA (left lower) with age in 96 TD participants, covarying for sex. Decreases of NAA with age were seen in many of the same areas. Sex-by-diagnosis interactions (right upper) for Glx covarying for age, diagnosis, and use of any psychotropic medication. Positive interactions were seen in centrum semiovale (CSO) and posterior thalamic radiations (PTR). Regions (right middle) where metabolites are higher (orange-red) or lower (cyan-blue) in male than female participants covarying for age and use of any psychotropic medication; 78 (63 male/15 female) ASD participants. Sites with sex-by-diagnosis in black. Posterior middle cingulate cortex (pMCC). Regions (right lower) where metabolites are higher or lower in

male than female participants covarying for age; 96 (69 male/27 female) YD participants. (For results elsewhere in brain and with other metabolites see Supplemental Figures S8–S11.)

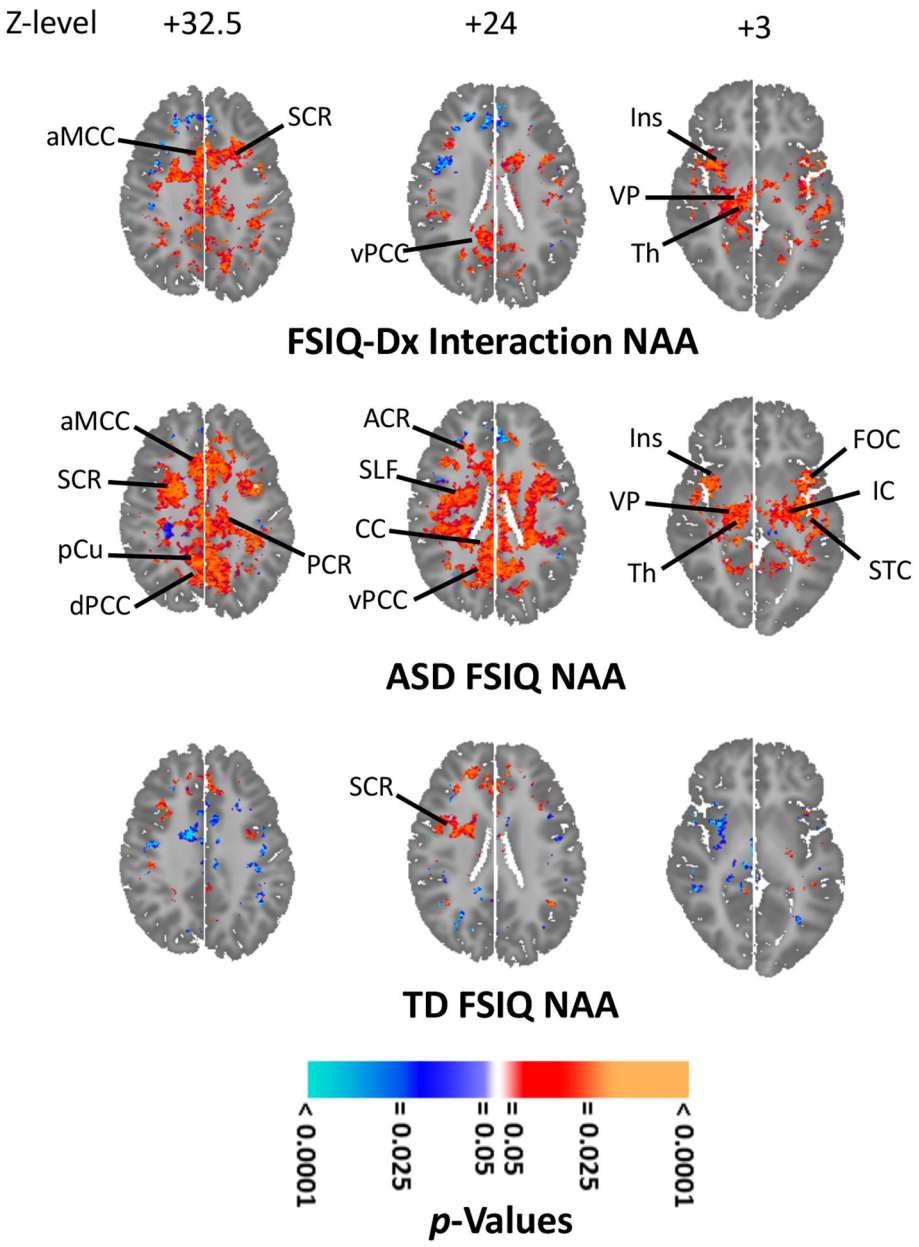

Figure 5.

Effects of full-scale intelligence quotient (FSIQ) on *N*-acetyl-compounds (NAA) levels in autistic spectrum disorder (ASD). FSIQ-by-diagnosis interactions (right upper; orange-red) were seen in SCR, aMCC, dPCC, ventral PCC (vPCC), Ins, ventral pallidum (VP), and thalamus (Th). (Covariates: age, sex, FSIQ, medication; 68 ASD, 93 TD.) NAA (right middle) correlated positively with FSIQ in IC, SCR, PCR, anterior corona radiata (ACR), superior longitudinal fasciculus (SLF), corpus callosum (CC), IC, aMCC, precuneus (pCu), dPCC, vPCC, Ins, frontal opercular cortex (FOC), superior temporal cortex (STC), VP, and Th. (Covarying age, sex, medication; 68 ASD.) For 93 TD, NAA (right lower) was little affected by FSIQ. (Covariates were age and sex. Elsewhere in brain NAA was unaffected by or correlated inversely with FSIQ; Supplemental Figure S14C.) All results corrected for

multiple comparisons using false discovery rate. For further findings including similar effects for other anatomic sections and other metabolites see Supplemental Results.

Table 1.

Participant Characteristics

	ASD (*n* = 78)	TD (*n* = 96)	ASD vs. TD	
	Mean (SD)	Mean (SD)	Statistic	*p*
Age (Years)	22.5 (13.9)	22.3 (12.3)	$t = 0.05$	0.908
Age Group (Child/Adult)	34/44	43/53	$\chi^2 = 0.02$	0.874
Sex (Female/Male)	15/63	27/69	$\chi^2 = 1.86$	0.173
SES[a] (Hollingshead Score)	49.2 (10.7)	51.8 (12.1)	$t = -0.11$	0.195
FSIQ[b] (points)	108.5 (25.6)	115.3 (12.4)	$t = -0.17$	0.046
ADOS Total (points)	11.4 (4.1)	--	--	--
Social Awareness	9.5 (3.8)	--	--	--
Restricted and Repetitive Behaviors	1.9 (1.6)	--	--	--
SRS Total (points)	87.8 (29.2)	20.1 (16.9)	$t = 1.45$	$<10^{-6}$
Social Awareness	10.9 (3.7)	4.7 (3.1)	$t = 2.92$	$<10^{-6}$
Social Cognition	16.3 (5.5)	3.1 (3.3)	$t = 1.48$	$<10^{-6}$
Social Communication	29.7 (10.2)	6.1 (6.5)	$t = 1.40$	$<10^{-6}$
Social Motivation	14.4 (5.9)	3.4 (3.1)	$t = 1.20$	$<10^{-6}$
Restricted Behavior	17 (6.8)	2.9 (3.5)	$t = 1.34$	$<10^{-6}$
Psychotropic Usage				
None	52	96	--	
Any	26	0	--	
antipsychotics	8[c]	0	--	
anticonvulsants	7[c]	0	--	
other mood stabilizers	2[c]	0	--	
SSRIs or SNRIs	11[c]	0	--	
other antidepressants	2[c]	0	--	
benzodiazepines	2[c]	0	--	
stimulants	9[c]	0	--	
dopaminergic agents	1[c]	0	--	

ADOS, Autism Diagnostic Observation Schedule (3); ASD, patients with autistic spectrum disorder; SNRI, serotonin–norepinephrine reuptake inhibitor; SRS, Social Responsiveness Scale (4); SSRI, selective serotonin-reuptake inhibitor; TD, typically developing control participants.

[a] Socioeconomic status based on Hollingshead

[b] Full-Scale Intelligence Quotient based on Wechsler

[c] Numbers do not sum to 26 due to polypharmacy